



# Electrochemical synthesis of a nanocomposite consisting of carboxy-modified multi-walled carbon nanotubes, polythionine and platinum nanoparticles for simultaneous voltammetric determination of myricetin and rutin

Chaoqiao Liu<sup>1</sup> · Jianzhi Huang<sup>1</sup> · Lishi Wang<sup>1</sup>

Received: 29 May 2018 / Accepted: 2 August 2018 / Published online: 16 August 2018  
© Springer-Verlag GmbH Austria, part of Springer Nature 2018

## Abstract

The authors describe a method for electrochemical synthesis of a nanocomposite consisting of carboxylated multi-walled carbon nanotubes, polythionine and platinum nanoparticles (denoted as cMWCNT@pTh@Pt). The composite was placed on a glassy carbon electrode (GCE) to obtain a sensor for simultaneous determination of myricetin and rutin by differential pulse voltammetry, with typical peak voltages of 0.16 and 0.34 V (vs. SCE). Under optimal conditions, the modified GCE has a linear response in the range of 0.01–15  $\mu\text{M}$  myricetin concentration range, and a 3 nM lower detection limit. For rutin, the data are 0.01–15  $\mu\text{M}$  and 1.7 nM, respectively. The sensor is selective, stable and reproducible. It was successfully applied to the simultaneous determination of myricetin and rutin in spiked juice samples, and satisfactory results were obtained.

**Keywords** Flavonoids · Nanocomposites sensor · Simultaneous determination · Electropolymerization · Electrodeposition · Conductive polymer · Electron mediator · Signal amplifier · Electrocatalytic oxidation · Synergistic effect

## Introduction

Myricetin and rutin are two typical natural flavonoids (Chart 1) [1], which have anti-oxidative, anti-bacterial and anti-tumor medical effects [2]. While the similar chemical structure and physical features, resulting in difficult to distinguish them [3, 4]. Therefore, it is a great challenge to construct a convenient, accurate and sensitive analytical method for simultaneous determination of myricetin and rutin in food and medicine field. Up to date, several reported methods such as chemiluminescence [5, 6], high performance liquid

chromatography [7, 8], spectrophotometry [9] and capillary electrophoresis [10] have been used for the myricetin and rutin detection. Although these methods are quite mature and widely used for flavonoids detection, while as electroactive compounds, both myricetin and rutin can be detected by electrochemical method, which is an instrumental simplicity, fast response and high sensitivity analytical method. However, the preparation of complex nanomaterial and poor stability for electrochemical method still need to be improved and optimized. Some flavonoid electrochemical sensors have been reported to detect myricetin [11–13] or rutin [14–17], simultaneous determination of myricetin and rutin has rarely been reported, due to their analogous chemical structure and electrochemical properties, causing an indistinguishable potential [4, 12]. Therefore, it was urgent and necessary to develop an electrochemical sensor that can realize simultaneous determination of myricetin and rutin.

Multi-walled carbon nanotubes (MWCNTs) as electrochemical signal amplification [18, 19] have been widely used in electroanalytical chemistry due to their unique properties such as excellent electrical conductivity, high surface area, high chemical stability and high mechanical strength [20–22]. Moreover, some groups functionalization of

---

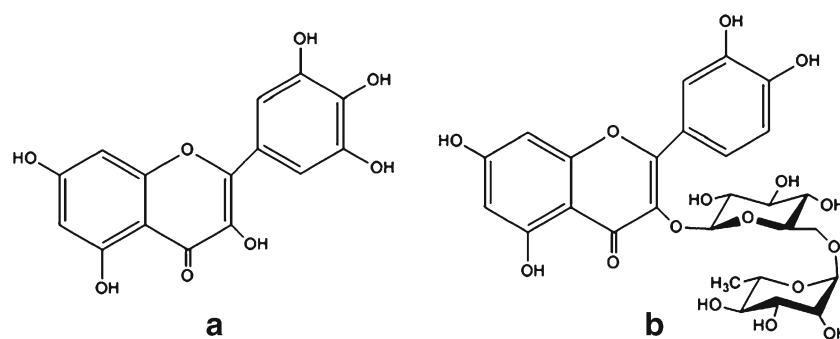
**Electronic supplementary material** The online version of this article (<https://doi.org/10.1007/s00604-018-2947-7>) contains supplementary material, which is available to authorized users.

---

✉ Jianzhi Huang  
hjanzhi0628@163.com

✉ Lishi Wang  
wanglsh@scut.edu.cn

<sup>1</sup> School of Chemistry and Chemical Engineering, South China University of Technology, Guangzhou 510641, People's Republic of China

**Chart 1** Chemical structures of myricetin (A) and rutin (B)

MWCNTs such as hydroxyl (–OH), carboxyl (–COOH), and carbonyl (–C=O) can make them combine with other nanomaterials more easily [23]. Polythionine as an excellent electron transfer mediator [24] with good redox reversibility and stability, which has been widely used in sensors fabrication [25, 26]. Platinum nanoparticles as a noble metal catalyst was introduced into electrochemical sensor for amplifying the electrochemical signal of flavonoids, attributing to it possesses superior conductivity and can improve electrocatalytic oxidation of phenolic hydroxyl especially for the polyhydroxy flavone compounds [27, 28].

In this work, we combined the advantages of cMWCNTs, polythionine and platinum nanoparticles through an electrostatic interaction between positive charge  $S^+$  of polythionine and negative charge  $-COO^-$  of the cMWCNTs. In addition, the existence of amine groups (–NH<sub>2</sub>) on the conductive polymers is beneficial to immobilize platinum nanoparticles [29]. Therefore, a three-layer nanocomposite including cMWCNTs, polythionine and Pt NPs was constructed for the simultaneously quantitative determination of rutin and myricetin, demonstrated wide linear detection ranges and low detection limits. Finally, the nanocomposite sensor was successfully applied to the real samples detection and got a satisfactory result.

## Experimental

### Chemicals and reagents

Rutin (98%, analytical grade), thionine (98%, analytical grade) and chloroplatinic acid hexahydrate (99.9%, analytical grade) were purchased from J&K Chemical (Beijing, China, [www.jkchemical.com](http://www.jkchemical.com)). Carboxylic multi-walled carbon nanotubes and myricetin (97%, analytical grade) were purchased from Aladdin Chemical Reagent Co. Ltd. (Shanghai, China, [www.aladdin-e.com](http://www.aladdin-e.com)). All other reagents were of analytical grade and used without further purification. 1.0 mmol dm<sup>-3</sup> rutin and 1.0 mmol dm<sup>-3</sup> myricetin were dissolved in 50 mL absolute ethanol and diluted with doubly distilled water to 100 mL, thus

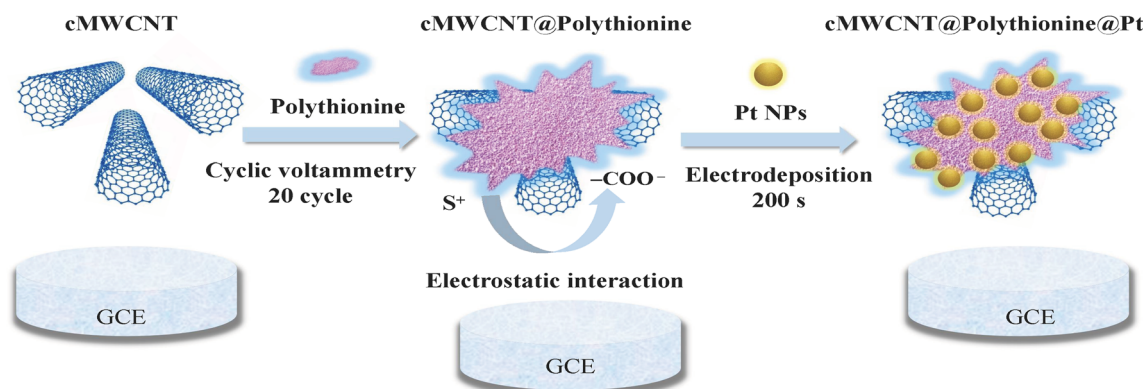
obtaining the stock solutions. Orange Juice was diluted with BR buffer (pH = 5.0) as a real sample for analysis. Prior to use, 0.01 g of cMWCNTs was dispersed in 20 mL of doubly distilled water and sonicated for 30 min to get a cMWCNTs aqueous solution (0.5 mg mL<sup>-1</sup>). Britton–Robinson (BR) buffer was prepared by mixing 0.04 mol dm<sup>-3</sup> of boric acid (0.618 g), phosphoric acid (680 μL) and acetic acid (572 μL) in 250 mL doubly distilled water, and then adjusted to the required pH with NaOH solution. All aqueous solutions were prepared with doubly distilled water.

### Fabrication of the cMWCNT@pTh@Pt nanocomposite sensor

A novel electrochemical synthesis strategy was used in the fabrication of the nanocomposite electrochemical sensor in Scheme 1. Prior to electrode modification, a bare glassy carbon electrode (3 mm in diameter) was firstly polished with 0.3 μm alumina powders, and then successively polished with 0.05 μm alumina powders. After polishing, the bare GCE was rinsing with absolute alcohol and doubly distilled water in an ultrasonic bath, and then was dried in nitrogen stream. 5 μL of 0.5 mg mL<sup>-1</sup> cMWCNTs aqueous solution was dropped onto the bare GCE surface, and then dried at room temperature, thus obtained cMWCNT/GCE. The electropolymerization of thionine was performed in 0.2 mmol dm<sup>-3</sup> thionine containing 0.1 mol dm<sup>-3</sup> H<sub>2</sub>SO<sub>4</sub> solution by cyclic voltammetry at a scan rate of 50 mV s<sup>-1</sup> between –0.4 V and +0.8 V for 20 cycles. After electropolymerization, a potentiostatic deposition method was used to obtain Pt nanoparticles in 0.2 mmol dm<sup>-3</sup> H<sub>2</sub>PtCl<sub>6</sub> solution containing 0.5 mol dm<sup>-3</sup> H<sub>2</sub>SO<sub>4</sub>, where a constant potential of –0.3 V (vs. Ag/AgCl) was applied to electrodeposit Pt NPs on the surface of polythionine for 200 s.

### Apparatus and method

Cyclic voltammetry (CV), electrochemical impedance spectroscopy (EIS) and differential pulse voltammetry (DPV) experiments were performed on a CHI 660E electrochemical workstation (Chenhua, Shanghai, China), a three-electrode configuration was used in all electrochemical experiments. In the



**Scheme 1** Fabrication of cMWCNT@pTh@Pt nanocomposite sensor

process of electrodeposition of Pt NPs, Ag/AgCl electrode was used as the reference electrode. While in the electrochemical measurements, saturated calomel electrode (SCE) was used as reference electrode, GCE was used as working electrode, platinum wire was used as counter electrode. If not mention, the potentials were all respect to SCE. For differential pulse voltammetry, amplitude was 0.05 V, pulse width was 0.05 s, pulse period was 0.5 s, increment was 0.005 V, potential range was from  $-0.1$  V to  $0.65$  V. EIS measurement was measured at  $5 \text{ mmol dm}^{-3}$  of  $\text{K}_3[\text{Fe}(\text{CN})_6]/\text{K}_4[\text{Fe}(\text{CN})_6]$  solution containing  $0.1 \text{ mol dm}^{-3}$  of KCl with a frequency range from  $0.1$  Hz to  $100$  kHz and  $50$  mV amplitude. Field emission scanning electron microscope (FE-SEM; Zeiss Ultra 55, Germany) was used to characterize the surface morphology of the modified electrodes. The working solution was deaerated with  $\text{N}_2$  for  $15$  min before the electrochemical measurements.

## Results and discussion

### The choice of materials for sensor preparation

The same as the conventional carbon nanomaterials (graphene, carbon quantum dots and carbon fiber), MWCNTs also have the advantages of excellent conductivity, large surface area and low toxicities. In addition, MWCNTs are multi-layer hollow and crooked tubular structure, which make MWCNTs possess more defects sites than other carbon nanomaterials. A large number of defect sites on MWCNTs will promote the functionalization of carboxyl groups. The pTh not only possesses good conductive ability like other common conductive polymers (polyaniline, polypyrrole and polythiophene), but also can serve as an electron mediator to promote the transfer rate of charges. In order to further improve the electrochemical performances of the cMWCNT@pTh nanocomposite, Pt NPs

were introduced to promote electrocatalytic oxidation of myricetin and rutin, which also show more excellent electrocatalytic performance than other noble metal nanoparticles (gold and silver). Therefore, a three-layer nanocomposite including cMWCNTs, pTh and PtNPs was constructed electrochemical sensor for sensitive detection of myricetin and rutin.

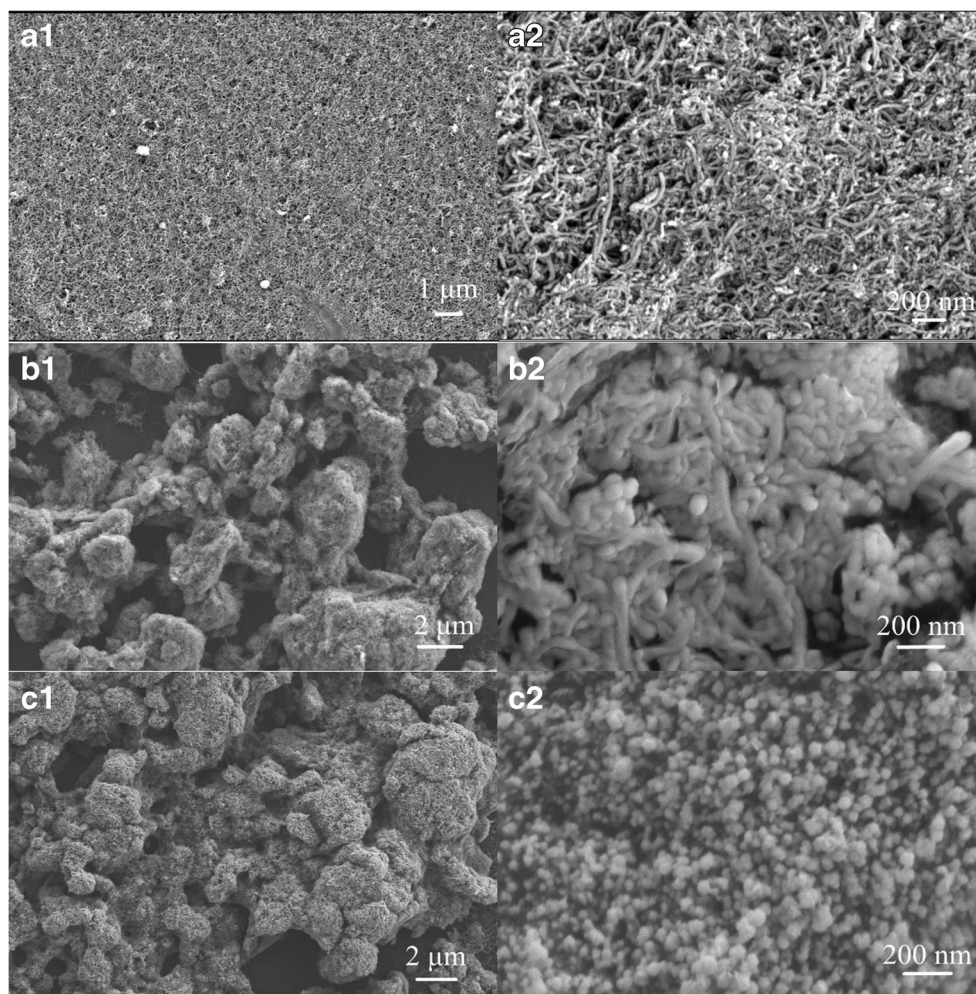
### Morphology and electrochemical characterization of the nanocomposite

Figure 1 A1 and A2 depicted SEM images at low and high magnification of the cMWCNTs, one-dimensional structure of cMWCNTs was easily observed on the electrode surface. However, when the polythionine was electropolymerized to the surface of cMWCNTs, three-dimensional structure of nanocomposite was formed. The cMWCNTs was coated by polythionine, a clear view of the polymer layer with a rough surface was obvious observed for cMWCNT@pTh nanocomposite in Fig. 1 B1 and B2. Subsequently, after the potentiostatic deposition of Pt NPs, Pt NPs were highly uniform distributed on the surface of polythionine (Fig. 1 C1 and C2). Therefore, three-dimensional cMWCNT@pTh@Pt nanocomposite was successfully fabricated by a layer-by-layer electrochemical synthesis strategy.

Figure 2a shows the cyclic voltammograms of different modified electrodes in  $5.0 \text{ mmol dm}^{-3}$   $\text{K}_4[\text{Fe}(\text{CN})_6]/\text{K}_3[\text{Fe}(\text{CN})_6]$  solution containing  $0.1 \text{ mol dm}^{-3}$  KCl. The redox-label  $[\text{Fe}(\text{CN})_6]^{3-/4-}$  displayed a reversible CV curve at the bare GCE. Obviously, after modification with polythionine and Pt nanoparticles successively, both the oxidation and reduction peaks current increased successively, indicated that both polythionine and Pt NPs can improve the electron transfer rate between electroactive species in solution and electrode surface. Figure 2b shows the EIS plots of different electrodes. A small semicircle at high frequencies was observed at the bare GCE. When cMWCNTs



**Fig. 1** SEM images at low and high magnification of cMWCNT/GCE (A1–2), cMWCNT@pTh/GCE (B1–2) and cMWCNT@pTh@Pt/GCE (C1–2)

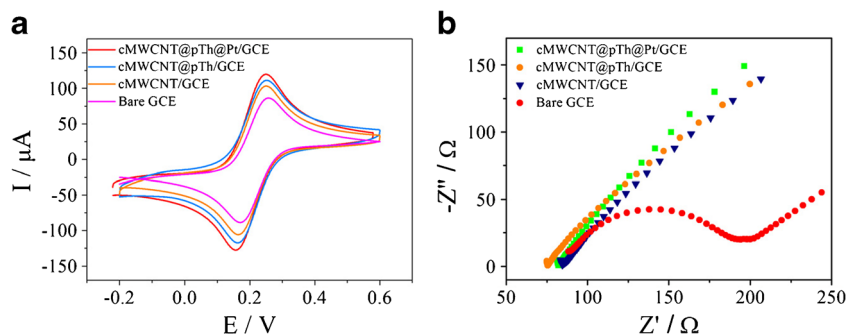


was modified on the GCE surface, it displayed a straight line in the Nyquist plot. The decrease of impedance was owing to the cMWCNTs can greatly enhance the electron transfer for  $[\text{Fe}(\text{CN})_6]^{3-/4-}$  probe [30, 31]. After modified the pTh and Pt NPs, the Nyquist plot still present a straight line, which demonstrated the modified electrode have an excellent electron transfer performance. Therefore, both the SEM images and electrochemical characterization proved the successfully fabrication of cMWCNT@pTh@Pt nanocomposite sensor.

### Electrochemical behavior of myricetin and rutin

The electrochemical behavior of myricetin and rutin at bare GCE, cMWCNT/GCE, cMWCNT@pTh/GCE, and cMWCNT@pTh@Pt/GCE were investigated by background-subtracted DPV in BR buffer (pH = 5.0) containing 0.5% ethanol. As shown in Fig. 3, compared with bare GCE, cMWCNT/GCE, and CMWCNT@pTh/GCE, two well-defined oxidation peaks of myricetin and rutin are

**Fig. 2** **a** CVs and **(b)** EIS of bare GCE, cMWCNT/GCE, cMWCNT@pTh/GCE and cMWCNT@pTh@Pt/GCE in 5.0 mM  $[\text{Fe}(\text{CN})_6]^{3-/4-}$  containing 0.1 M KCl



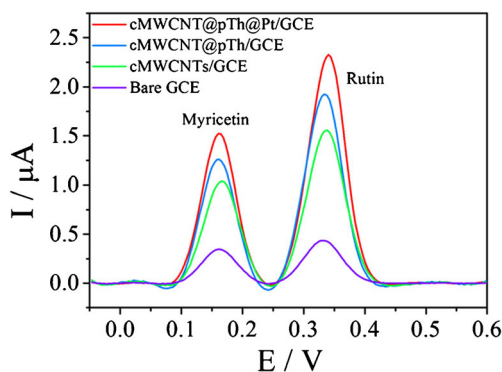


**Fig. 3** Background-subtracted DPVs of  $10 \mu\text{mol dm}^{-3}$  myricetin and  $10 \mu\text{mol dm}^{-3}$  rutin at bare GCE, cMWCNT/GCE, cMWCNT@pTh/GCE and cMWCNT@pTh@Pt/GCE in BR buffer (pH = 5.0)

respectively presented at 0.16 V and 0.34 V on the cMWCNT@pTh@Pt/GCE, which are well distinguished with each other and the potential differences are large enough to simultaneously determine the myricetin and rutin. Moreover, oxidation peaks current of myricetin and rutin on cMWCNT@pTh@Pt/GCE were much stronger than cMWCNT/GCE and cMWCNT@pTh/GCE. The electrochemical surface area can be calculated from the Randle–Sevcik equation:  $I_p = 2.69 \times 10^5 AD^{1/2} n^{3/2} \nu^{1/2} C$  [32]. Here,  $A$  is the surface area of the electrode ( $\text{cm}^2$ ),  $n$  is the number of electrons involved in the redox reaction,  $D$  is the diffusion coefficient of the molecule in solution ( $6.67 \times 10^{-6} \text{ cm}^2 \text{ s}^{-1}$  for ferricyanide),  $C$  is the concentration of ferricyanide and  $\nu$  is the scan rate. The surface area of cMWCNT/GCE, cMWCNT@pTh/GCE and cMWCNT@pTh@Pt/GCE are calculated as  $0.2046 \text{ cm}^2$ ,  $0.2079 \text{ cm}^2$  and  $0.2323 \text{ cm}^2$ , which are higher than the surface area of the bare GCE ( $0.0707 \text{ cm}^2$ ). In Fig. 3, the current responses of myricetin and rutin on cMWCNT/GCE, cMWCNT@pTh/GCE and cMWCNT@pTh@Pt/GCE are  $10.67 \mu\text{A}$  and  $15.84 \mu\text{A}$ ,  $13.27 \mu\text{A}$  and  $19.79 \mu\text{A}$ ,  $15.41 \mu\text{A}$  and  $23.39 \mu\text{A}$ , respectively. Therefore, the electrochemical sensitivity of the myricetin on cMWCNT/GCE, cMWCNT@pTh/GCE and cMWCNT@pTh@Pt/GCE are calculated as 5.215, 6.383 and  $6.634 \mu\text{A } \mu\text{M}^{-1} \text{ cm}^{-2}$ . The sensitivities of the rutin on cMWCNT/GCE, cMWCNT@pTh/GCE and cMWCNT@pTh@Pt/GCE are calculated as 7.742, 9.519 and  $10.07 \mu\text{A } \mu\text{M}^{-1} \text{ cm}^{-2}$ . In summary, the cMWCNT@pTh@Pt/GCE is the highest sensitivity for simultaneous determination of myricetin and rutin.

These results attribute to the synergistic effect among cMWCNTs, pTh and Pt NPs: cMWCNTs as a good signal amplifier possess excellent conductivity, which can be easily combined by the thionine through an electrostatic interaction between positive charge  $\text{S}^+$  of polythionine and negative charge  $-\text{COO}^-$  of the cMWCNTs. Furthermore, the amine groups ( $-\text{NH}_2$ ) of the conductive polymers is beneficial to electrodeposit Pt NPs. Therefore, such a three

dimensional sandwich structure can combine the electrochemical signal amplification ability of cMWCNTs and fast charge transfer performance of polythionine, which have a synergistic promoting effect for the platinum nanoparticles to electrocatalytic oxidation of myricetin and rutin. Therefore, the cMWCNT@pTh@Pt nanocomposite sensor can be successfully applied in simultaneous determination of myricetin and rutin.

### The optimal conditions of myricetin and rutin detection

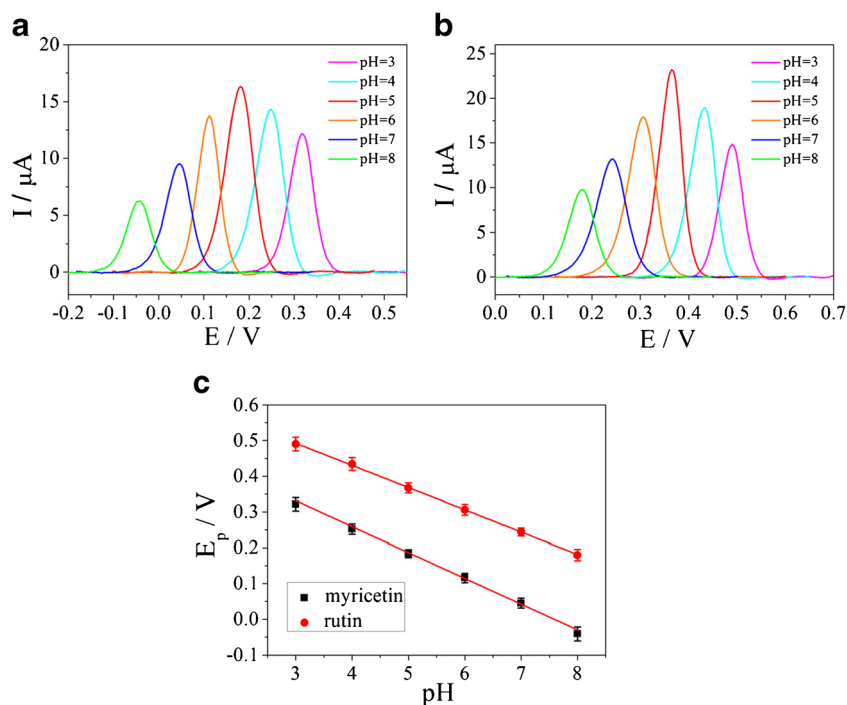
The effects of electropolymerization cycles of polythionine and electrodeposition time of Pt NPs for the simultaneous determination of  $10 \mu\text{mol dm}^{-3}$  myricetin and rutin in BR buffer (pH = 5.0) were investigated by DPV. As shown in Fig. S1A (Electronic Supplementary Material), the oxidation peaks current of myricetin and rutin are attained the maximum at 20 cycles, which was chosen as the optimal electropolymerization cycles in subsequent determination. As shown in Fig. S1B, the maximum of oxidation peaks current of myricetin and rutin emerge at the 200 s. Therefore, Pt electrodeposition time of 200 s was used in latter experiments.

The effect of solution pH values on the electrochemical responses of myricetin and rutin at the cMWCNT@pTh@Pt nanocomposite sensor was investigated with the pH range from 3 to 8 by DPV (Fig. 4a, b). In Fig. S1C, the maximum oxidation peaks current of myricetin and rutin emerge at the pH 5.0, which is chosen as the optimal working pH in the following measurements. Furthermore, the peak potentials and pH of solution showed linear relationships (Fig. 4c), with the regression equations expressed as:  $E_{\text{pa}} = -0.0684\text{pH} + 0.5389$  ( $R = 0.9978$ ) and  $E_{\text{pa}} = -0.0623\text{pH} + 0.6796$  ( $R = 0.9996$ ) for myricetin and rutin respectively. Moreover, the slopes of the  $E_{\text{pa}}$ -pH plots are  $68.4 \text{ mV/pH}$  and  $62.3 \text{ mV/pH}$ , all close to the theoretical value of  $59.2 \text{ mV/pH}$ , indicating the numbers of transferring electron and proton involved in the electrode reaction are same. The corresponding reaction mechanisms [4, 12] for myricetin and rutin are shown in Scheme S1.

### The effect of scan rate

In Fig. S2A and 2B, CVs of  $10 \mu\text{mol dm}^{-3}$  myricetin and rutin in BR buffer (pH = 5.0) were respectively recorded in various scan rates ranging from 30 to  $300 \text{ mV s}^{-1}$  on cMWCNT@pTh@Pt nanocomposite sensor. As shown in Fig. S2C and 2D, both the oxidation peaks current of myricetin and rutin presented linear relationships with the square root of the scan rates, where the linear regression equations were expressed as  $I_{\text{pa}} (\mu\text{A}) = 2.221\nu^{1/2} (\text{mV s}^{-1})^{1/2} - 10.15$  ( $R = 0.9983$ ) and  $I_{\text{pa}} (\mu\text{A}) = 2.546\nu^{1/2} (\text{mV s}^{-1})^{1/2} - 11.27$  ( $R = 0.9987$ ) respectively.

**Fig. 4** Background-subtracted DPVs of  $10 \mu\text{mol dm}^{-3}$  myricetin (a) and rutin (b) in BR buffer (pH = 5.0) at different pH values on the cMWCNT@pTh@Pt nanocomposite sensor. c The relationship of pH values vs. oxidation peaks potential of myricetin and rutin



These results demonstrated that the electrochemical redox process of myricetin and rutin are typical diffusion controlled process, and indicated the myricetin and rutin are quickly oxidized and reduced on the nanocomposite sensor.

### Quantitative determination of myricetin and rutin

In Fig. 5a, the individual quantitative determination of myricetin was performed by DPV at different concentrations of myricetin in BR buffer (pH = 5.0) with the presence of  $0.5 \mu\text{mol dm}^{-3}$  rutin. As shown in Fig. 5b, there are two different detection ranges for myricetin in  $0.01\text{--}1 \mu\text{mol dm}^{-3}$  and  $1\text{--}15 \mu\text{mol dm}^{-3}$ , and the linear regression equations are  $I_p$  ( $\mu\text{A}$ ) =  $5.227c$  ( $\mu\text{mol dm}^{-3}$ ) +  $1.039$  ( $R = 0.9945$ ) and  $I_p$  ( $\mu\text{A}$ ) =  $0.9343c$  ( $\mu\text{mol dm}^{-3}$ ) +  $5.478$  ( $R = 0.9915$ ), respectively. Fig. 5c showed DPVs observed at different concentrations of rutin with the presence of  $0.5 \mu\text{mol dm}^{-3}$  myricetin. The oxidation peak current of rutin increase linearly with concentration ranges of  $0.01\text{--}1 \mu\text{mol dm}^{-3}$  and  $1\text{--}15 \mu\text{mol dm}^{-3}$  in Fig. 5d, and the linear regression equations are  $I_p$  ( $\mu\text{A}$ ) =  $8.989c$  ( $\mu\text{mol dm}^{-3}$ ) +  $0.8965$  ( $R = 0.9974$ ) and  $I_p$  ( $\mu\text{A}$ ) =  $1.545c$  ( $\mu\text{mol dm}^{-3}$ ) +  $8.496$  ( $R = 0.9947$ ), respectively.

The simultaneous quantitative determination of myricetin and rutin was performed by DPV under optimal conditions. Fig. 5e shows the DPVs of myricetin and rutin under different concentrations. There are two different detection ranges both observed for myricetin and rutin in  $0.01\text{--}1 \mu\text{mol dm}^{-3}$  and  $1\text{--}15 \mu\text{mol dm}^{-3}$  (Fig. 5f, g), and the linear regression equations of high concentration ( $1\text{--}15 \mu\text{mol dm}^{-3}$ ) for myricetin and rutin

are expressed as  $I_p$  ( $\mu\text{A}$ ) =  $0.9726c$  ( $\mu\text{mol dm}^{-3}$ ) +  $5.3914$  ( $R = 0.9938$ ) and  $I_p$  ( $\mu\text{A}$ ) =  $1.627c$  ( $\mu\text{mol dm}^{-3}$ ) +  $7.189$  ( $R = 0.9975$ ), respectively. And the linear regression equations of myricetin and rutin in the low concentration ( $0.01\text{--}1 \mu\text{mol dm}^{-3}$ ) are  $I_p$  ( $\mu\text{A}$ ) =  $5.288c$  ( $\mu\text{mol dm}^{-3}$ ) +  $0.4848$  ( $R = 0.9946$ ) and  $I_p$  ( $\mu\text{A}$ ) =  $7.897c$  ( $\mu\text{mol dm}^{-3}$ ) +  $0.7703$  ( $R = 0.9935$ ) respectively. Based on the signal-to-noise ratio of 3 ( $S/N = 3$ ), the detection limits for myricetin and rutin are calculated to be  $3.8 \text{ nmol dm}^{-3}$  and  $1.7 \text{ nmol dm}^{-3}$  ( $S/N = 3$ ) respectively. At low concentrations of myricetin and rutin at the electrode surface, which were rapidly depleted and converted into products by electrocatalytic oxidation, this resulting in a high sensitivity of the electrode response and a bigger slope of linear equation. While at high concentrations, the electrochemical reaction process of myricetin and rutin at electrode surface needs a longer time. And the possibility of the electrode surface was polluted by the reaction products, results in a small slope of the linear equation. Therefore, the nanocomposite sensor exhibited two different linear ranges at different concentration ranges. And the slope of the linear equation at low concentration ranges was used to calculate the LOD values.

Compared with reported electrochemical sensors for determination of myricetin or rutin (Table 1), the new sensor can realize the simultaneous determination of myricetin and rutin, presented a wider linear detection range with a lower detection limit, which can be attributed to its excellent conductivity, high catalytic

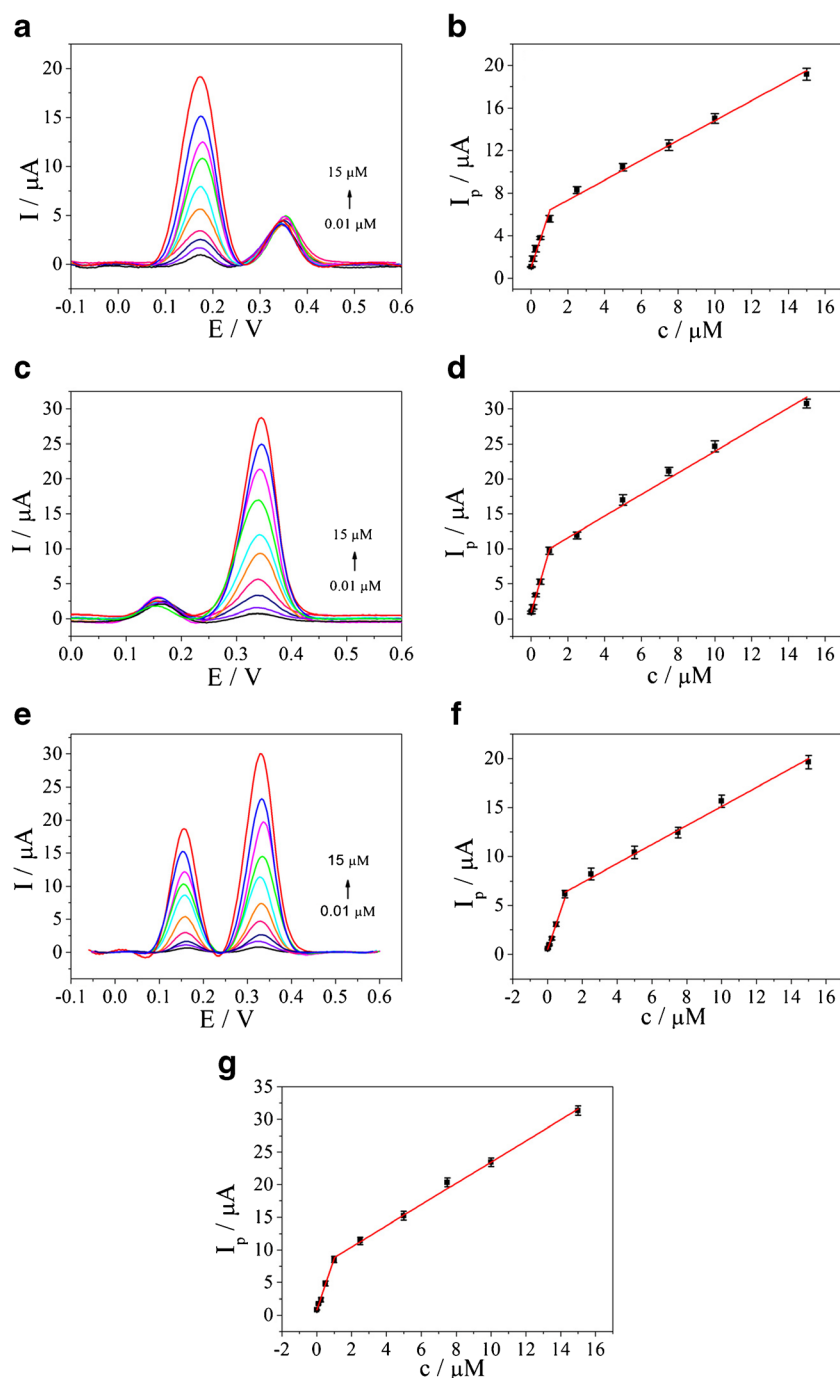


**Fig. 5** **a** Background-subtracted DPVs of myricetin at different concentrations (0.01–15  $\mu\text{mol dm}^{-3}$ ) in BR buffer (pH = 5) with the presence of 0.5  $\mu\text{mol dm}^{-3}$  rutin at the cMWCNT@pTh@Pt/GCE. **b** Linear relationship between oxidation peak current and concentration of myricetin. **c** Background-subtracted DPVs of rutin at different concentrations (0.01–15  $\mu\text{mol dm}^{-3}$ ) in BR buffer (pH = 5) with the presence of 0.5  $\mu\text{mol dm}^{-3}$

myricetin at the cMWCNT@pTh@Pt/GCE. **d** Linear relationship between oxidation peak current and concentration of rutin. **e** Background-subtracted DPVs of myricetin and rutin at different concentrations both from 0.01 to 15  $\mu\text{mol dm}^{-3}$  in BR buffer (pH = 5.0) at cMWCNT@pTh@Pt/GCE. And the corresponding linear relationships of oxidation peaks current for myricetin (**f**) and rutin (**g**) with different concentrations

performance and large electrochemical active surface. In addition, the fabrication of our nanocomposite sensor was more controllable and convenient through the strategy of electrochemical synthesis.

### Selectivity, reproducibility and stability

In order to evaluate the selectivity of the cMWCNT@pTh@Pt nanocomposite sensor, the possible interferences from various



**Table 1** Comparison of detection performances with other reported sensors for the determination of myricetin or rutin

Electrode	Method	Linear range ( $\mu\text{mol dm}^{-3}$ )	Limit of detection ( $\text{nmol dm}^{-3}$ )	Reference
Cu-CS/MWCNTs/GCE	DPV	Myricetin: — Rutin: 0.05–100	— 10	[33]
MIP/GO–MWCNTs/GCE	DPV	Myricetin: — Rutin: 0.01–1	— 5	[17]
PSSA/CNTs/MBT/Au/GCE	DPV	Myricetin: — Rutin: 0.8–10	— 1.8	[34]
AuNPs/MWCNTs/GCE	SWV	Myricetin: 0.05–40 Rutin: —	12 —	[11]
$\beta$ -CD–Au@PTCA–SWCNHs/GCE	DPV	Myricetin: 0.01–10 Rutin: 0.01–10	3.8 4.4	[12]
Polyfurfural film/GCE	DPV	Myricetin: 0.05–10 Rutin: 0.001–10	10 0.025	[4]
cMWCNT@pTh@Pt/GCE	DPV	Myricetin: 0.01–15 Rutin: 0.01–15	3.8 1.7	This work

100-fold inorganic compounds and 10-fold organic compounds have been investigated by DPV in this work. As indicated in Table 2, there are not obvious signal changes of the oxidation peaks current for myricetin and rutin, demonstrates that the nanocomposite sensor is suitable for the simultaneous determination of myricetin and rutin with superior selectivity. Moreover, we have ever tried to study the effect of much higher concentration of organic interferences like ascorbic, L-cysteine, citric acid and glucose, which caused obvious influence for the detection of target analyte. Actually, some flavonoids have similar chemical structure with myricetin and rutin, resulting in an indistinguishable redox peak potential and large interference.

**Table 2** Effects of various possible interferences on the oxidation peaks current signal of  $10 \mu\text{mol dm}^{-3}$  myricetin and rutin in BR (pH = 5.0) solution at cMWCNT@pTh@Pt nanocomposite sensor. Sample responses are expressed as a confidence interval of 95% probability ( $n = 3$ )

Interference	Concentration ( $\text{mmol dm}^{-3}$ )	Current signal change (%)	
		Myricetin	Rutin
CaCl <sub>2</sub>	1	1.98 ± 0.16	1.09 ± 0.28
K <sub>3</sub> PO <sub>4</sub>	1	−1.81 ± 0.26	−2.03 ± 0.31
MgSO <sub>4</sub>	1	−0.08 ± 0.08	3.02 ± 0.42
NaHCO <sub>3</sub>	1	−0.12 ± 0.14	−0.46 ± 0.14
Zn(Ac) <sub>2</sub>	1	1.40 ± 0.19	−3.13 ± 0.28
H <sub>2</sub> O <sub>2</sub>	1	−4.02 ± 0.44	1.59 ± 0.21
Citric acid	0.1	2.53 ± 0.22	−3.36 ± 0.33
Ascorbic acid	0.1	−3.13 ± 0.14	−4.06 ± 0.56
Uric acid	0.1	−4.46 ± 0.25	3.40 ± 0.21
Glucose	0.1	−3.79 ± 0.41	−3.91 ± 0.34
Tartaric acid	0.1	4.41 ± 0.26	2.77 ± 0.14
Cystine	0.1	−4.17 ± 0.37	1.15 ± 0.09

For example, we have ever tried to simultaneous distinguish the peak potential of quercetin, myricetin and rutin through an electrochemistry method but failed.

Reproducibility of the electrochemical sensors is another significant factor in their practical applications. To investigate the reproducibility of nanocomposite sensor, five modified electrodes were fabricated and applied to the simultaneous determination of myricetin and rutin under the same conditions. The relative standard deviation (RSD) of the oxidation peaks current of myricetin and rutin were calculated to be  $3.13 \pm 0.49\%$  and  $1.45 \pm 0.39\%$  for myricetin and rutin respectively, confirmed satisfactory reproducibility. The stability was evaluated after the sensors were stored at 4 °C in a refrigerator for 1 month. The oxidation peaks current of myricetin and rutin still retained 91.2 and 95.9% of their initial responses respectively, indicating excellent stability. Therefore, with excellent selectivity, reproducibility and stability, the sensor is promising for the simultaneous determination of myricetin and rutin.

### Analytical application for real samples

The analytical reliability and application potential of the cMWCNT@pTh@Pt nanocomposite sensor was evaluated by real samples detection in this work. As active components, myricetin and rutin are often added into juice to make them possess healthy function [2]. Therefore, orange juice samples were chosen as real samples for simultaneously quantitative analysis through a standard-addition technique, and three parallel experiments were performed on all determinations. The results were shown in Table 3, the average recoveries of myricetin and rutin were between 92.2 and 100.4%, and the RSD values were less than 6.2%, suggesting that the sensor can be successfully applied for the simultaneous determination of myricetin and rutin in real samples.



**Table 3** The recovery of myricetin and rutin in real orange juice samples

	Added ( $\mu\text{mol dm}^{-3}$ )	Found <sup>a</sup> ( $\mu\text{mol dm}^{-3}$ )	Recovery (%)	RSD (%)
Myricetin	0.5	0.50 ± 0.06	100.4	6.1
	1	0.98 ± 0.01	98.0	4.7
	5	4.82 ± 0.11	96.4	6.2
	10	9.28 ± 0.24	92.8	5.9
Rutin	0.5	0.46 ± 0.03	92.2	2.8
	1	0.97 ± 0.07	97.0	4.5
	5	4.84 ± 0.14	96.8	3.6
	10	9.59 ± 0.34	95.9	5.0

<sup>a</sup> Sample responses are expressed as a confidence interval of 95% probability ( $n = 3$ )

## Conclusions

In summary, a novel cMWCNT@pTh@Pt nanocomposite sensor based on electrochemical synthesis strategy was fabricated for simultaneous determination of myricetin and rutin. Such a three-dimensional nanocomposite exhibits excellent electrocatalytic ability for the sensitive detection of myricetin and rutin due to the synergetic effects of cMWCNT (superior electrical conductivity), pTh (excellent electron transfer mediator) and Pt (good electrocatalytic performance). However, the preparation of complex and expensive nanomaterials limits its practical application. The synthesis strategy of this nanocomposite sensor need to be further optimized for the economic detection of myricetin and rutin in practical sample analysis.

**Acknowledgments** This work was financially supported by the National Natural Science Foundation of China (Grant Nos. 21475046, 21427809, 21645004).

**Compliance with ethical standards** The author(s) declare that they have no competing interests.

## References

- Seifried HE, Anderson DE, Fisher EI, Milner JA (2007) A review of the interaction among dietary antioxidants and reactive oxygen species. *J Nutr Biochem* 18:567–579
- Wojdylo A, Oszmianski J, Czemerys R (2007) Antioxidant activity and phenolic compounds in 32 selected herbs. *Food Chem* 105: 940–949
- Lu QH, Ba CD, Chen DY (2008) Investigating noncovalent interactions of rutin-serum albumin by capillary electrophoresis-frontal analysis. *J Pharm Biomed* 47:888–891
- Huang JZ, Shen XL, Hu Q, Ma Y, Bai SL, Yue GQ, Yu XT, Zeng Q, Wang LS (2016) High sensitivity simultaneous determination of myricetin and rutin using a polyfurfural film modified glassy carbon electrode. *RSC Adv* 6:95435–95441
- Yang D, Li H, Li Z, Hao Z, Li J (2010) Determination of rutin by flow injection chemiluminescence method using the reaction of luminol and potassium hexacyanoferrate(III) with the aid of response surface methodology. *Luminescence : J Biol Chem* 25: 436–444
- Jiang HL, He YZ, Zhao HZ, Hu YY (2004) Determination of chlorogenic acid and rutin in cigarettes by an improved capillary electrophoresis indirect chemiluminescence system. *Anal Chim Acta* 512:111–119
- Surowiec I, Nowik W, Trojanowicz M (2007) Post-column deprotonation and complexation in HPLC as a tool for identification and structure elucidation of compounds from natural dyes of historical importance. *Microchim Acta* 162:393–404
- Wang Y, Cao J, Weng JH, Zeng S (2005) Simultaneous determination of quercetin, kaempferol and isorhamnetin accumulated human breast cancer cells, by high-performance liquid chromatography. *J Pharm Biomed* 39:328–333
- Xu H, Li Y, Tang HW, Liu CM, Wu QS (2010) Determination of rutin with UV-vis spectrophotometric and laser-induced fluorimetric detections using a non-scanning spectrometer. *Anal Lett* 43: 893–904
- He JL, Yang Y, Yang X, Liu YL, Liu ZH, Shen GL, Yu RQ (2006)  $\beta$ -Cyclodextrin incorporated carbon nanotube-modified electrode as an electrochemical sensor for rutin. *Sensors Actuators B Chem* 114:94–100
- Hajian R, Yusof NA, Faragi T, Shams N (2014) Fabrication of an electrochemical sensor based on gold nanoparticles/carbon nanotubes as nanocomposite materials: determination of myricetin in some drinks. *PLoS One* 9:1–7
- Ran X, Yang L, Zhang J, Deng G, Li Y, Xie X, Zhao H, Li CP (2015) Highly sensitive electrochemical sensor based on beta-cyclodextrin-gold@3, 4, 9, 10-perylene tetracarboxylic acid functionalized single-walled carbon nanohorns for simultaneous determination of myricetin and rutin. *Anal Chim Acta* 892:85–94
- Munir S, Park SY (2016) Liquid crystal-based DNA biosensor for myricetin detection. *Sensors Actuators B Chem* 233:559–565
- Yang B, Bin D, Zhang K, Du Y, Majima T (2018) A seed-mediated method to design N-doped graphene supported gold-silver nanohorns sensor for rutin detection. *J Colloid Interface Sci* 512: 446–454
- Zou CE, Zhong J, Li S, Wang H, Wang J, Yan B, Du Y (2017) Fabrication of reduced graphene oxide-bimetallic PdAu nanocomposite for the electrochemical determination of ascorbic acid, dopamine, uric acid and rutin. *J Electroanal Chem* 805:110–119
- Wang Z, Yu G, Xia J, Zhang F, Liu Q (2018) One-step synthesis of a methylene blue@ZIF-8-reduced graphene oxide nanocomposite and its application to electrochemical sensing of rutin. *Microchim Acta* 185:279–286
- Yang L, Yang J, Xu B, Zhao F, Zeng B (2016) Facile preparation of molecularly imprinted polypyrrole-graphene-multiwalled carbon nanotubes composite film modified electrode for rutin sensing. *Talanta* 161:413–418
- Akter R, Rahman MA, Rhee CK (2012) Amplified electrochemical detection of a cancer biomarker by enhanced precipitation using horseradish peroxidase attached on carbon nanotubes. *Anal Chem* 84:6407–6415
- Sun W, Wang X, Zhu H, Sun X, Shi F, Li G, Sun Z (2013) Graphene-MnO<sub>2</sub> nanocomposite modified carbon ionic liquid electrode for the sensitive electrochemical detection of rutin. *Sensors Actuators B Chem* 178:443–449
- Cesarino I, Cesarino V, Lanza MR (2013) Carbon nanotubes modified with antimony nanoparticles in a paraffin composite electrode: simultaneous determination of sulfamethoxazole and trimethoprim. *Sensors Actuators B Chem* 188:1293–1299
- Gong K, Wu X, Zhao G, Wang X (2017) Tribological properties of polymeric aryl phosphates grafted onto multi-walled carbon nanotubes as high-performances lubricant additive. *Tribol Int* 116:172–179

22. Moraes FC, Cabral MF, Mascaro LH, Machado SAS (2011) The electrochemical effect of acid functionalisation of carbon nanotubes to be used in sensors development. *Surf Sci* 605:435–440
23. Wahab R, Khan ST, Ahmad J, Ansari SG, Musarrat J, Al-Khedhairy AA (2017) MWCNTs functionalization and immobilization with anti- Brucella antibody; towards the development of a nanosensor. *Vacuum* 146:623–632
24. Gao Q, Cui X, Yang F, Ma Y, Yang X (2003) Preparation of poly(thionine) modified screen-printed carbon electrode and its application to determine NADH in flow injection analysis system. *Biosens Bioelectron* 19:277–282
25. Dempsey E, Diamond D, Collier A (2004) Development of a biosensor for endocrine disrupting compounds based on tyrosinase entrapped within a poly(thionine) film. *Biosens Bioelectron* 20: 367–377
26. Ahammad AJS, Rahman MM, Xu GR, Kim S, Lee JJ (2011) Highly sensitive and simultaneous determination of hydroquinone and catechol at poly(thionine) modified glassy carbon electrode. *Electrochim Acta* 56:5266–5271
27. Liu Z, Xue Q, Guo Y (2017) Sensitive electrochemical detection of rutin and isoquercitrin based on SH-beta-cyclodextrin functionalized graphene-palladium nanoparticles. *Biosens Bioelectron* 89: 444–452
28. Yao YY, Zhang L, Wang ZF, Xu JK (2014) Electrochemical determination of quercetin by self-assembled platinum nanoparticles/poly(hydroxymethylated-3,4-ethylenedioxythiophene) nanocomposite modified glassy carbon electrode. *Chin Chem Lett* 25:505–551
29. Neouze MA, Schubert U (2008) Surface modification and functionalization of metal and metal oxide nanoparticles by organic ligands. *Monatsh Chem* 139:183–195
30. Lu J, Liu S, Ge S, Yan M, Yu J, Hu X (2012) Ultrasensitive electrochemical immunosensor based on Au nanoparticles dotted carbon nanotube-graphene composite and functionalized mesoporous materials. *Biosens Bioelectron* 33:29–35
31. Fang YS, Huang XJ, Wang LS, Wang JF (2015) An enhanced sensitive electrochemical immunosensor based on efficient encapsulation of enzyme in silica matrix for the detection of human immunodeficiency virus p24. *Biosens Bioelectron* 64:324–332
32. Bard AJ, Faulkner LR (2001) *Electrochemical methods: fundamentals and applications*. Wiley, New York
33. Gholivand MB, Mohammadi-Behzad L, Hosseinkhani H (2016) Application of a Cu-chitosan/multiwalled carbon nanotube film-modified electrode for the sensitive determination of rutin. *Anal Biochem* 493:35–43
34. Arvand M, Farahpour M, Ardaki MS (2018) Electrochemical characterization of in situ functionalized gold organosulfur self-assembled monolayer with conducting polymer and carbon nanotubes for determination of rutin. *Talanta* 176:92–101